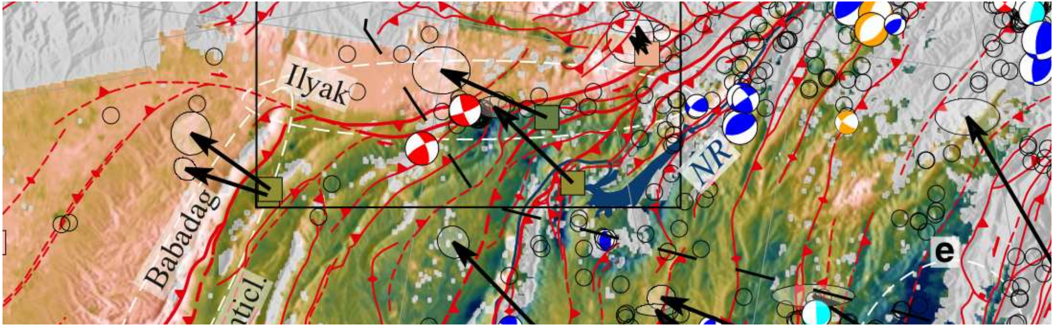

High-resolution InSAR rate maps showcase tectonic and anthropogenic processes in the Tajik Basin, Central Asia

S. Metzger, Ł. Gagała, L. Ratschbacher, B. Schurr, M. Lazecky, Y. Maghsoudi

GFZ Helmholtz Centre Potsdam

Pamir Tectonics & Motivation

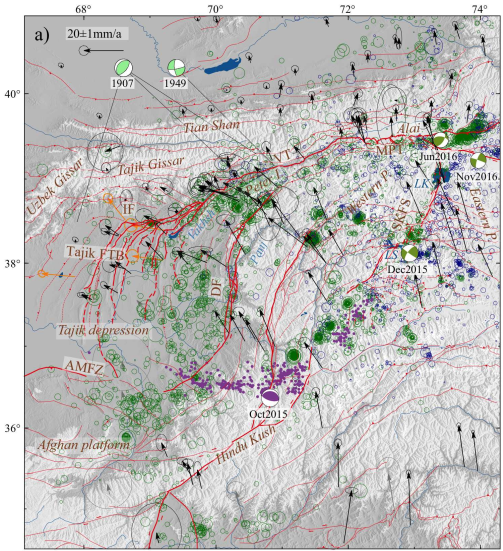

Situated at the northwestern end of the Himalayan syntax, the Pamir is a unique place to study continental collision, causing the building and subsequent destruction of mountains. On its northward advance, the Pamir separated the former Tarim-Tajik basin, while the Tian Shan acts as a buttress in the North.

GNSS rates exhibit westward crustal extrusion of the W-Pamir, causing E-W shortening in the Tajik fold-and-thrust belt, where low-friction, evaporitic décollements separate the sedimentary sheets from basement rock. Abundant seismicity along the northern and northwestern rim hosts M6-7 earthquakes every ∼10 years, the last example being the 2015 M7.2 Central Pamir earthquake that ruptured the sinistral Sarez Karakul faults (SKFS).

We present high-resolution InSAR rates of the greater Pamir to deepen our kinematic knowledge and identify active structures. A particular focus is upon the Tajik basin, where we have a profound knowledge of the geological structures in terms of geometry and rheology, but not of their recent activity.

(in prep.)

InSAR rate maps using pre-processed interferograms and SBAS time-series analysis

(LiCSAR – Lazecky et al.; LiCSBAS – 2020, Morishita et al., 2020)

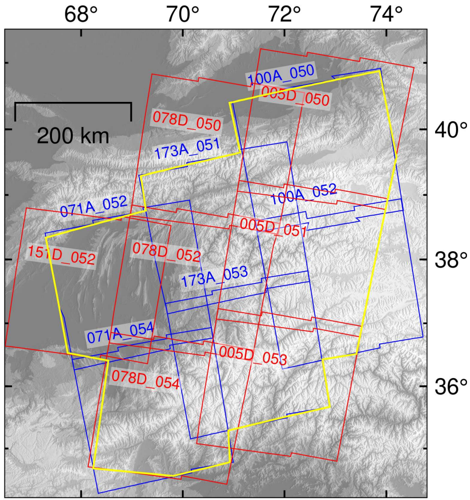

(in prep.)

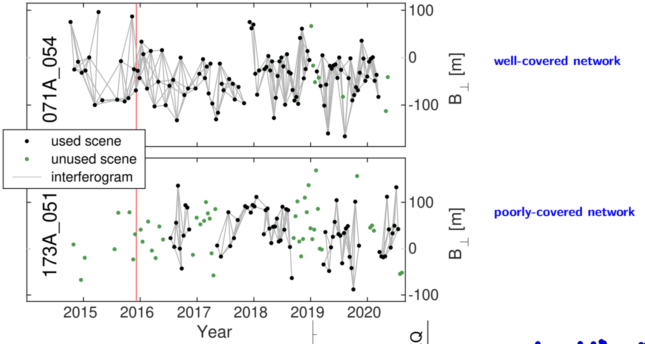

We derived InSAR rate maps of six ascending and seven descending radar frames of the Greater Pamir area to obtain high-resolution (400 m) deformation rates in line-of-sight.

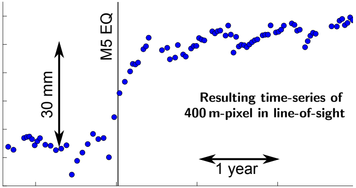

Tying LOS Rates to GNSS Data

Following Qi Ou's PhD thesis (Uni Oxford, in prep.) we corrected each rate map with a linear ramp to optimize the fit to the horizontal GNSS data and the frame overlap along-track. For three successive InSAR frames $I1$ to $I3$ and the co-located GNSS rates $G1$ to $G3$ (collapsed into line-of-sight) both conditions are met with

$$\begin{bmatrix} I1 - I2 \\ I2 - I3 \\ I1 - G1 \\ I2 - G2 \\ I3 - G3 \end{bmatrix} = \begin{bmatrix} x & y & 1 & -x & -y & -1 & 0 & 0 & 0 \\ 0 & 0 & 0 & x & y & 1 & -x & -y & -1 \\ x & y & 1 & 0 & 0 & 0 & 0 & 0 & 0 \\ 0 & 0 & 0 & x & y & 1 & 0 & 0 & 0 \\ 0 & 0 & 0 & 0 & 0 & 0 & x & y & 1 \end{bmatrix} \cdot \begin{bmatrix} a_1 \\ b_1 \\ c_1 \\ \dots \\ a_3 \\ b_3 \\ c_3 \end{bmatrix}$$

where x,y being the column and row index numbers of the merged pixel index frame and a,b,c the linear ramp parameters to be inverted for. The weights of the along-track overlap pixels are weighted with $(\sigma(I1) + \sigma(I2))^{-1}$. The combined weights of GNSS and InSAR are

$$\sqrt{\frac{m}{n}}(\sigma(I1) + \sigma(G1))^{-1},$$

with $\sigma(I1)$ being the standard deviation of all pixels within the search radius of a GNSS data point and $\sigma(G1)$ being collapsed into line-of-sight (LOS). The term is normalized by the number of InSAR data points m and GNSS data points n.

Tying InSAR rate maps to the Eurasian reference frame

InSAR uncertainties

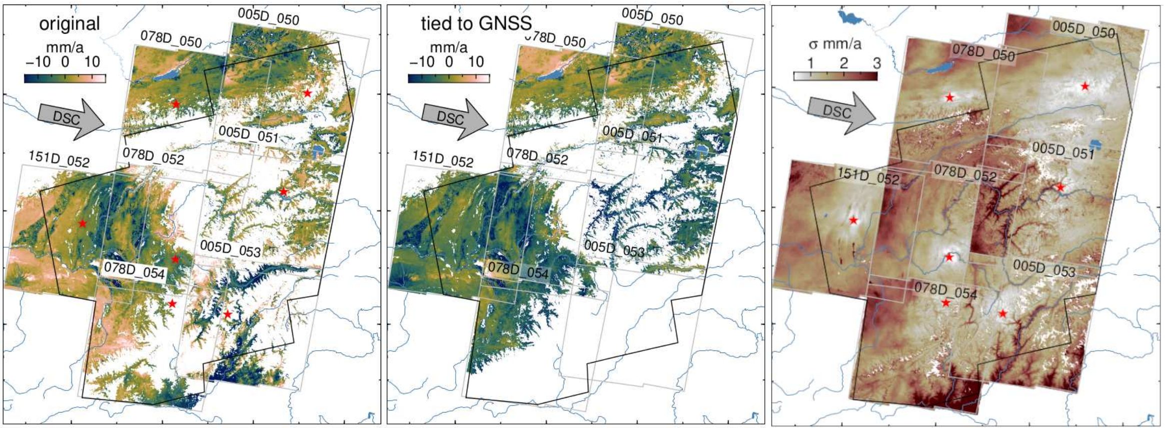

Individual rate maps with independent reference points (red stars) were tied to the Eurasian-stable GNSS reference frame and decomposed in East and Up rates by constraining the North component to spatially interpolated GNSS rates. Original LiCSBAS rate uncertainties (right) were scaled based on GNSS uncertainties and misfits.

(in prep.)

From LOS to East and Up Rates

Rate maps in two view angles can further be decomposed into East and a sub-Vertical direction:

$$V_{LOS} = \left[-\cos(\phi)\sin(\theta) \quad \sqrt{1 - \sin^2(\theta)\cos^2(\phi)} \right] \cdot \begin{bmatrix} V_E \\ V_N \end{bmatrix}$$

Each InSAR rate pixel is weighted by its standard deviation. The associated uncertainties $\sigma(V_E)$ and $\sigma(V_{UN})$ are calculated by the design matrix G and the squared uncertainty matrix Σ via $cov(p) = [G^T cov(d)^{-1} G]^{-1}$, where the diagonal terms of $cov(p)$ are the variances, respectively squared uncertainties, of V_E and V_{UN}.
We decompose V_{UN} using interpolated GNSS constraints on the North component and solved for the Up component,

$$V_U = \frac{V_{UN} \cdot \sqrt{1 - \sin^2(\theta)\cos^2(\phi)}}{\cos(\theta)} - V_N \frac{\sin(\phi)\sin(\theta)}{\cos(\theta)}$$

The corresponding uncertainties were calculated by replacing the rates with the uncertainties in the above formula.

Rate uncertainty maps

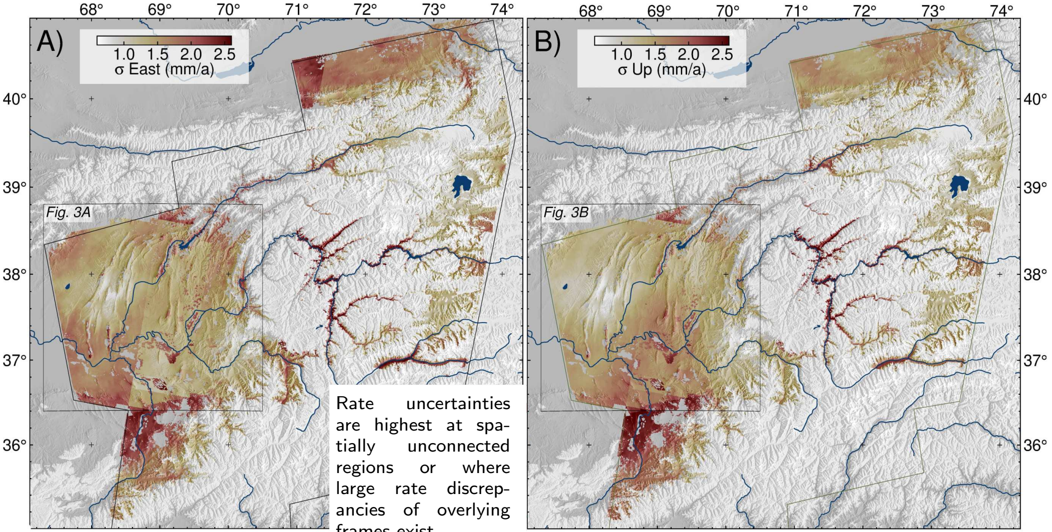

Rate uncertainties are highest at spatially unconnected regions or where large rate discrepancies of overlying frames exist.

(in prep.)

East and Up rates of the Greater Pamir

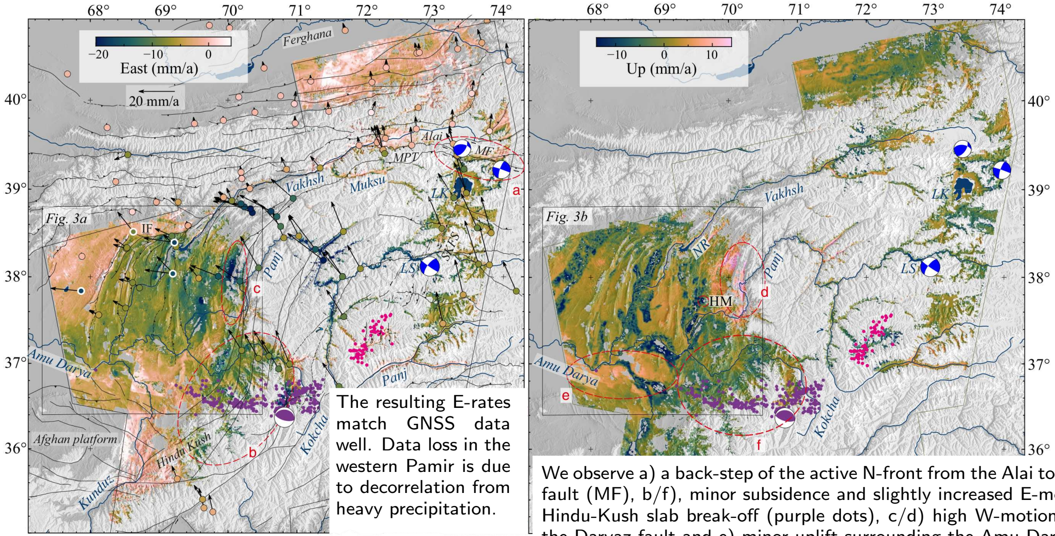

The resulting E-rates match GNSS data well. Data loss in the western Pamir is due to decorrelation from heavy precipitation.

We observe a) a back-step of the active N-front from the Alai to the Markansu fault (MF), b/f), minor subsidence and slightly increased E-motion near the Hindu-Kush slab break-off (purple dots), c/d) high W-motion and uplift at the Darvaz fault and e) minor uplift surrounding the Amu Darya river bed.

(in prep.)

East and Up rates of the Tajik Depression

Complex interaction of shallow- and deep-rooted processes

E-W shortening

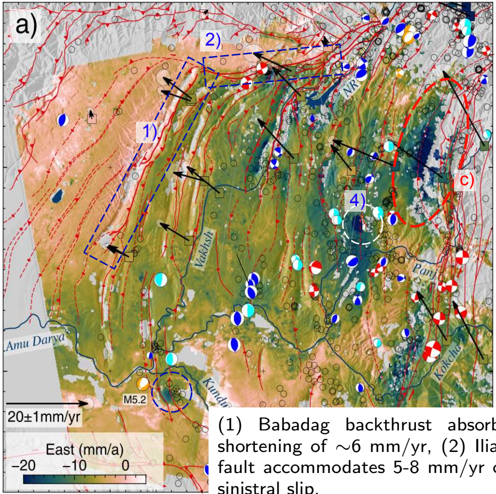

(1) Babadag backthrust absorbs shortening of ~6 mm/yr, (2) Iliak fault accommodates 5-8 mm/yr of sinistral slip.

(Mostly) Shallow processes

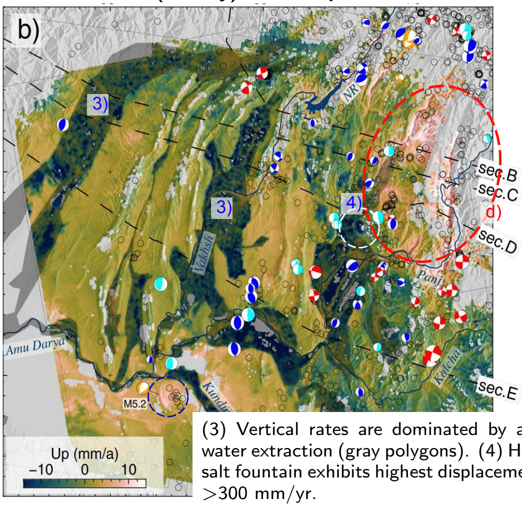

(3) Vertical rates are dominated by agricultural water extraction (gray polygons). (4) Hoja Mumin salt fountain exhibits highest displacement rates of >300 mm/yr.

(in prep.)

Rates along cross section “C” (interpretation in progress!)

Topography

East rates

Up rates

Geological cross sections (Gagała et al., 2020)

(in prep.)

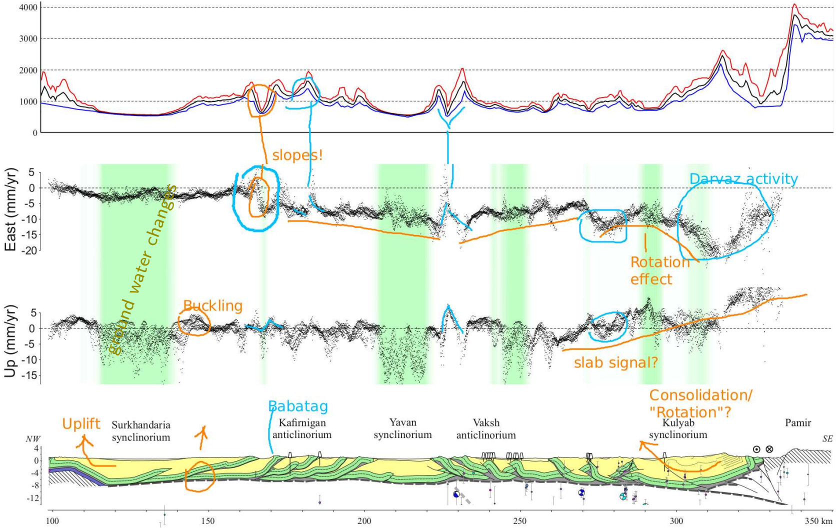

Faulting vs. folding

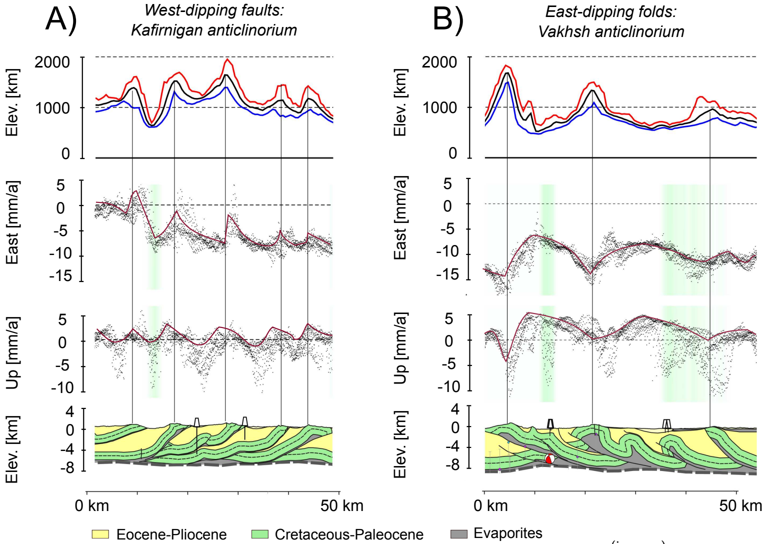

(in prep.)

A) East / Up **out of** phase, **sharp** rate changes

B) East / Up **in** phase, **smooth** rate changes

Ilyak fault, near Dushanbe

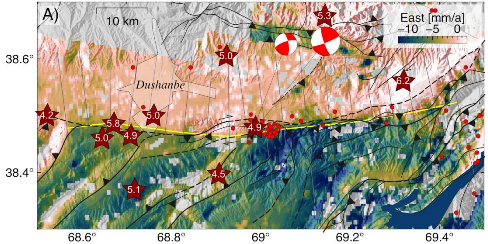

Earthquakes since 1950 of Hakimov et al.(2021)

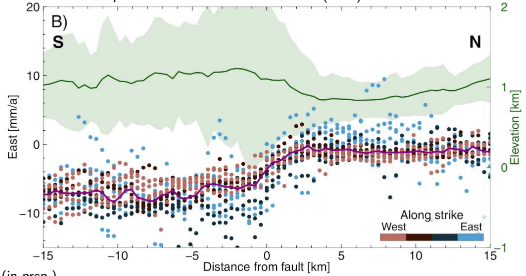

(in prep.)

- slip ∼5-8 mm/a
- locking <1 km, probably creep
- horizontal escape on evaporitic décollements

⇒ Is strain accumulated in the bedrock?

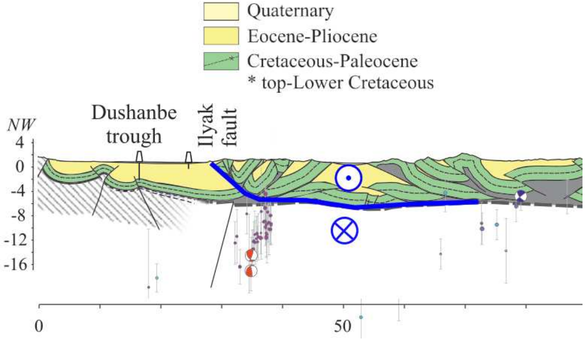

NW-SE Geological cross-section of Gagała et al., 2020